ELSEVIER

Journal of Alloys and Compounds 239 (1996) 83–87

Journal of
ALLOYS
AND COMPOUNDS

Subsolidus phase relations of the ternary La–Co–Al system

Yongquan Guo[a], Jingkui Liang[a,b], Weihua Tang[a], Yanming Zhao[a], Guanghui Rao[a]

[a]*Institute of Physics, Chinese Academy of Sciences, P.O. Box 603, Beijing 100080, People's Republic of China*
[b]*International Centre for Materials Physics, Academia Sinica, Shenyang 110015, People's Republic of China*

Received 6 November 1995; in final form 3 December 1995

Abstract

The subsolidus phase relations of the La–Co–Al ternary system have been investigated by X-ray powder diffraction. The following ternary intermetallic compound and solid solutions were observed: $LaCoAl_4$, $LaCo_{5-x}Al_x$ ($x \leq 1$), $LaAl_{2-x}Co_x$ ($x \leq 0.6$) and $LaCo_{13-x}Al_x$ ($x \leq 3$). For the $LaCo_{13-x}Al_x$ solid solution, when $x \leq 2.7$, the crystal structure is cubic $NaZn_{13}$ type and the space group is $Fm3c$, $Z = 8$. At $x = 3$, there is a structural transition from the cubic $NaZn_{13}$ type to the tetragonal $Ce_2Ni_{17}Si_9$ type (space group $I4/mcm$, $Z = 4$). The subsolidus phase relations of the ternary La–Co–Al system can be divided into 18 three-phase, six two-phase and four single-phase regions.

Keywords: La–Co–Al system; Phase diagram; Isothermal section; Ternary intermetallic compounds

1. Introduction

$LaCo_{13}$ has the highest 3d metal content of any known rare earth–transition metal intermetallic compound. Its T_c is 1318 K and its magnetic induction at room temperature is 13 kG [1,2]. But, because of its cubic symmetry structure, it is unlikely to have an appreciable magnetic anisotropy. Hence, it would be important to search for 1:13 intermetallic compounds with lower symmetry. Several researchers have made efforts to improve the magnetic anisotropy of $LaCo_{13}$-based intermetallic compounds by elemental substitution [3] and different annealing treatments. According to various reports [4–7], up to now a lowered symmetry (tetragonal or orthorhombic) has been observed in the $R(Co,Ga)_{13}$ ($R = La, Ce, Pr$), $La(Co,Si)_{13}$, $La(Fe,Al)_{13}$ and $La(Fe,Si)_{13}$ systems. To our knowledge, there is no report on the subsolidus phase relations of the La–Co–Al ternary system. In this system, there exist many well-known magnetic intermetallic compounds, such as 1:1, 1:2, 1:3, 1:5, and 1:13. It will be of significance for the research and possible application of these compounds to investigate the phase relations in the La–Co–Al ternary system. Hence, we have systematically investigated the subsolidus phase relations in this system.

2. Experimental procedure

The La–Co–Al samples (116 experimental samples) were prepared by argon arc melting of appropriate amounts of the starting materials. The purity of the starting materials was better than 99.9%. To ensure the homogeneity of the samples, the ingots were turned upside down and melted several times. The weight loss of the samples was less than 1% during arc melting. Using the reported eutectic or peritectic reaction temperature of the binary compounds in the binary systems La–Co [8], Co–Al [9–12] and Al–La [9–12], the annealing temperatures of our samples were selected close to the above-mentioned temperatures. A temperature of 1073 K has been regarded as suitable when the eutectic or peritectic reaction temperatures are higher than this temperature. Otherwise the annealing temperature was selected at 773 K (see Table 3). As to the annealing method, the samples were wrapped with Ta foil and annealed at 1073 K for one month and 773 K for two months in evacuated quartz tubes.

A Guinier-de Wolff focusing camera with Co Kα radiation ($\lambda = 1.7903$ Å) was used to examine the samples before and after annealing. The phase identifications were performed by comparing diffraction lines

SSDI 0925-8388(95)02194-9

with JCPDS cards. The XRD intensity data of structural transition sample $LaCo_{10}Al_3$ were collected by a Rigaku automatic X-ray diffractometer with Cu $K\alpha_1$ radiation and graphite monochromator (λ = 1.5405 Å), operating at step-scan mode with a step of $2\theta = 0.02°$. High purity Si was added to the samples as an internal standard to correct the 2θ position for precise determination of lattice constants. The lattice constants were calculated by a standard least-squares method.

3. Experimental results and discussion

In the binary La–Co system, there are six kinds of binary compound [8]. These are La_3Co, La_xCo_{1-x} ($x = 0.54$), La_2Co_3, La_2Co_7 (α and β), $LaCo_5$ and $LaCo_{13}$. The La_xCo_{1-x} ($x = 0.54$) compound has been defined in Ref. [13] as $La_2Co_{1.7}$. For La_2Co_7, the polymorph transition temperature is 1073 K. However, under our present experimental conditions, β-La_2Co_7 was not observed. The existence of $LaCo_2$ was reported in Ref. [14], whereas elsewhere [15] $LaCo_2$ was not observed. The samples $LaCo_{2-x}Al_x$ ($x = 0$–0.6) with compositions have been investigated by X-ray powder diffraction. However, $LaCo_2$ was not observed under our experimental conditions. Another binary compound, La_4Co_3, reported in Ref. [16] was also not observed in our experiments.

For the binary Al–La system, six kinds of binary compound have been reported [9–12], i.e. La_3Al, LaAl, $LaAl_2$, $LaAl_3$, and $LaAl_4$ (high temperature and low temperature phase) and $LaAl_x$. According to the selected annealing temperature, the $LaAl_4$ (HT) and $LaAl_x$ compounds should not be observed. The $LaAl_4$ (LT) compound was defined as La_3Al_{11} in Ref. [17]. Hansen [9] had reported another binary compound, La_2Al_3, in the Al–La binary system. However, the later work of Buschow and coworker [17,18] and the assessed Al–La phase diagram of Gschneidner et al. [19] made it clear that the La_2Al_3 compound does not exist. Five kinds of binary compound have been observed under our experimental conditions. These were La_3Al, LaAl, $LaAl_2$, $LaAl_3$ and La_3Al_{11}.

In the binary Co–Al system, according to Refs. [9–12], there are four kinds of intermetallic compound. These are AlCo, Al_5Co_2, $Al_{13}Al_4$ and Al_9Co_2. For the AlCo compound, a homogeneity region exists in the range 47 to 59 at.% Al. All of these compounds have been observed in our diffraction analysis. Pearson [20] listed a questionable high temperature $AlCo_3$ phase with an ordered cubic ($L1_2$) structure isotypic

Table 2
List of planar spacings, observed and calculated diffraction intensities and the result of indexes of intermetallic compound $LaCo_{10}Al_3$

h k l	d_{obs} (Å)	d_{cal} (Å)	I_{obs}	I_{cal}
1 1 2	4.0755	4.0759	3	5
2 0 0	4.0422	4.0426	9	11
2 1 1	3.4524	3.4526	6	4
2 0 2	3.3185	3.3188	15	13
0 0 4	2.9060	2.9062	10	6
2 2 0	2.8538	2.8536	9	8
1 1 4	2.5905	2.5907	20	23
2 2 2	2.5649	2.5651	31	35
3 1 0	2.5566	2.5567	16	19
2 0 4	2.3595	2.3597	28	30
3 1 2	2.3402	2.3403	100	100
2 1 5	1.9554	1.9556	31	31
3 2 3	1.9407	1.9408	64	60
0 0 6	1.9373	1.9353	5	5
4 1 1	1.9335	1.9365	45	40
3 1 4	1.9195	1.9196	4	3
4 0 2	1.9090	1.9091	3	2
3 3 0	1.9055	1.9057	9	7
1 1 6	1.8348	1.8350	14	11
3 3 2	1.8107	1.8108	7	6
4 2 0	1.8078	1.8079	12	10
4 0 4	1.6593	1.6594	17	15
2 2 6	1.6037	1.6038	5	7
3 3 4	1.5935	1.5938	6	5
5 1 0	1.5855	1.5856	14	11
3 1 6	1.5441	1.5442	9	8
4 2 4	1.5350	1.5351	10	12
5 1 2	1.5296	1.5297	9	10
0 0 8	1.4530	1.4531	3	2
4 4 0	1.4292	1.4293	3	2
1 1 8	1.4082	1.4083	4	4
4 0 6	1.3986	1.3987	5	4
5 1 4	1.3918	1.3919	10	7
4 4 2	1.3878	1.3879	7	5
5 3 0	1.3864	1.3866	2	3
3 3 6	1.3585	1.3586	8	9
6 0 0	1.3474	1.3475	2	1
6 1 1	1.3205	1.3206	1	1
4 4 4	1.2825	1.2825	1	2
6 2 0	1.2783	1.2784	2	2
4 1 7	1.2672	1.2673	5	6
5 2 5	1.2616	1.2612	4	4
6 1 3	1.2572	1.2573	7	6
5 3 4	1.2514	1.2514	1	1

Results obtained by Rietveld powder diffraction profile fitting techniques.

Table 1
Variations in lattice parameter and unit volume vs. Al content in $LaCo_{13-x}Al_x$ compounds

x	0	0.3	0.6	0.9	1.2	1.5	1.8	2.1	2.4	2.7	3.0*	3.0*
a (Å)	11.345(2)	11.332(3)	11.354(7)	11.372(5)	11.383(1)	11.391(4)	11.399(1)	11.424(3)	11.460(1)	11.473(4)	8.085(1)	11.434(1)
V (Å^3)	1460.28(1)	1455.30(5)	1463.95(3)	1471.10(8)	1474.96(5)	1478.19(4)	1481.19(3)	1491.03(8)	1505.01(1)	1510.34(6)	759.89(9)	1519.79(9)

* At $x = 3$ the lattice constants of the tetragonal structure are $a = 8.085(1)$ Å (for cubic lattice $a_c = \sqrt{2}a = 11.434(1)$ Å), $c = 11.624(8)$ Å; the unit cell volume is 759.89(9) Å^3 (the double is 1519.79(9) Å^3); the linear equation of the lattice parameter vs. Al content is $a = 11.3452 + 0.0497x$ (x = Al content).

Table 3
List of phase identifications for various composition alloys in the La–Co–Al ternary system

No.	La (at.%)	Co (at.%)	Al (at.%)	Phase identification	Annealing temperature (K)
1–10	7.14	73.57–92.86	0–19.29	$LaCo_{13}$(c)	1073
11	7.14	71.43	21.43	$LaCo_{13}$(t)*	1073
12–16	7.14	64.29–70	22.86–28.57	$LaCo_{13}$(t) + $LaCo_5^{(s)}$ + $AlCo^{(s)}$	1073
17	7.14	50	42.86	$LaAl_2^{(s)}$ + La_2Co_3 + $AlCo^{(s)}$	773
18	7.14	42.86	50	$LaAl_2^{(s)}$ + $AlCo^{(s)}$	1073
19	7.14	35.71	57.15	$AlCo^{(s)}$ + $LaCoAl_4$	1073
20	7.14	28.57	64.29	$AlCo^{(s)}$ + $LaCoAl_4$ + Al_9Co_2	1073
21	4	22	74	$Al_{13}Co_4$ + Al_9Co_2 + $LaCoAl_4$	1073
22	6	6	88	Al_9Co_2 + La_3Al_{11} + Al	773
23	16.7	66.6	16.7	$LaCo_5^{(s)}$	1073
24	16.7	50	33.3	$AlCo^{(s)}$ + $LaAl_2^{(s)}$ + La_2Co_3	773
25	16.7	33.3	50	$AlCo^{(s)}$ + $LaAl_2^{(s)}$	1073
26	16.7	16.7	66.6	$LaCoAl_4$	1073
27	16.7	83.3	0	$LaCo_5$	1073
28	60	20	20	$La_2Co_{1.7}$ + LaAl + La_3Al	773
29	40	40	20	$LaAl_2^{(s)}$ + La_2Co_3 + $La_2Co_{1.7}$	773
30	40	20	40	$LaAl_2^{(s)}$ + $La_2Co_{1.7}$ + LaAl	773
31	16	4	80	La_3Al_{11} + Al_9Co_2	1073
32	20	4	76	La_3Al_{11} + Al_9Co_2 + $LaCoAl_4$	1073
33	24	4	72	$LaAl_3$ + $LaAl_2$ + $LaCoAl_4$	1073
34	28	4	68	$LaAl_3$ + $LaAl_2$ + $LaCoAl_4$	1073
35	33.3	60	6.7	$AlCo^{(s)}$ + $LaCo_5^{(s)}$ + La_2Co_3	773
36	33.3	53.4	13.3	$AlCo^{(s)}$ + La_2Co_3 + $LaAl_2^{(s)}$	773
37	10.53	89.47	0	$LaCo_{13}$(c) + $LaCo_5$	1073
38	10.53	80	9.47	$LaCo_{13}^{(s)}$(c) + $LaCo_5^{(s)}$	1073
39	10.53	69.47	20	$LaCo_{13}$(t) + $LaCo_5^{(s)}$	1073
40	10.53	60	29.47	$AlCo^{(s)}$ + $LaCo_5^{(s)}$ + La_2Co_3	773
41	10.53	49.47	40	La_2Co_3 + $LaAl_2^{(s)}$ + $AlCo^{(s)}$	773
42	10.53	37.47	52	$LaAl_2^{(s)}$ + $AlCo^{(s)}$	1073
43	10.53	28	61.47	$AlCo^{(s)}$ + $LaCoAl_4$	1073
44	10.53	18	71.47	Al_9Co_2 + $LaCoAl_4$	1073
45	10.53	9.47	80	La_3Al_{11} + Al_9Co_2	1073
46	10.53	0	89.47	La_3Al_{11} + Al	773
47	7.14	26	66.86	$AlCo^{(s)}$ + $LaCoAl_4$ + Al_5Co_2	1073
48	7.14	20	72.86	$LaCoAl_4$ + $Al_{13}Co_4$ + Al_9Co_2	1073
49	7.14	12	80.86	Al_9Co_2 + La_3Al_{11}	1073
50	0	28.57	71.43	Al_5Co_2	1073
51	0	23.53	76.47	$Al_{13}Co_4$	1073
52	0	81.82	18.18	Al_2Co_9	1073
53	4	48	48	$AlCo^{(s)}$ + $LaAl_2^{(s)}$	1073
54	4	54	42	$AlCo^{(s)}$ + $LaCo_5^{(s)}$	1073
55	4	10	86	Al + Al_9Co_2 + La_3Al_{11}	773
56	33.3	66.7	0	La_2Co_7 + La_2Co_3	773
57	33.3	62.7	4	La_2Co_3 + $LaCo_5^{(s)}$ + La_2Co_7	773
58	33.3	58.7	8	La_2Co_3 + $LaCo_5^{(s)}$ + $AlCo^{(s)}$	773
59–63	33.3	30–54.7	12–36.7	$LaAl_2^{(s)}$ + La_2Co_3 + $AlCo^{(s)}$	773
64–69	33.3	0–20	46.7–66.7	$LaAl_2^{(s)}$	1073
70	16.7	61.3	22	La_2Co_3 + $LaCo_5^{(s)}$ + $AlCo^{(s)}$	773
71	16.7	55.3	28	$AlCo^{(s)}$ + La_2Co_3	773
72	16.7	46	37.3	La_2Co_3 + $LaAl_2^{(s)}$ + $AlCo^{(s)}$	773
73	16.7	40	43.3	La_2Co_3 + $LaAl_2^{(s)}$ + $AlCo^{(s)}$	773
74	16.7	28	55.3	$LaAl_2^{(s)}$ + $AlCo^{(s)}$	773
75	16.7	23.3	60	$LaAl_2^{(s)}$ + $AlCo^{(s)}$ + $LaCoAl_4$	773
76	18	72	10	La_2Co_7 + $LaCo_5^{(s)}$	773
77	24	66	10	La_2Co_7 + $LaCo_5^{(s)}$ + La_2Co_3	773
78	16.7	77.3	6	$LaCo_5^{(s)}$	1073
79	24	48	28	La_2Co_3 + $LaAl_2^{(s)}$ + $AlCo^{(s)}$	773
80	26	26	48	$LaAl_2^{(s)}$ + $AlCo^{(s)}$	1073
81	8	16	76	Al_9Co_2 + $LaCoAl_4$ + La_3Al_{11}	1073
82–84	2–10	4–6	86–92	Al + La_3Al_{11} + Al_9Co_2	773
85	4	18	70	Al_9Co_2 + $LaCoAl_4$	1073
86	4	26	70	Al_5Co_2 + $LaCoAl_4$	1073
87	18	8	74	La_3Al_{11} + $LaCoAl_4$	1073
88	22.2	77.8	0	La_2Co_7	1073

Table 3 (*Continued*)

No.	La (at.%)	Co (at.%)	Al (at.%)	Phase identification	Annealing temperature (K)
89	22	54	24	$AlCo^{(s)} + La_2Co_3 + LaAl_2^{(s)}$	773
90	33.3	33.3	33.3	$LaAl_2^{(s)} + La_2Co_3 + AlCo^{(s)}$	773
91	66	26	8	$La_3Co + La_3Al + La_2Co_{1.7}$	773
92	68	6	26	$LaAl + La_3Al + La_2Co_{1.7}$	773
93	50	0	50	LaAl	773
94	48	44	8	$La_2Co_3 + LaAl_2^{(s)} + La_2Co_{1.7}$	773
95	48	26	26	$LaAl + LaAl_2^{(s)} + La_2Co_{1.7}$	773
96	58	34	8	$LaAl + La_3Al + La_2Co_{1.7}$	773
97	54	46	0	$La_2Co_{1.7}$	773
98	57.14	42.86	0	$La_2Co_{1.7} + La_3Co$	773
99	40	60	0	La_2Co_3	773
100	52	12	36	$LaAl + La_2Co_{1.7} + La_3Al$	773
101	42	8	50	$LaAl + LaAl_2^{(s)}$	773
102	29.3	0	70.7	$LaAl_2 + LaAl_3$	773
103	4	90	6	$Co + LaCo_{13}^{(s)}(c)$	1073
104–105	2–4	68–74	24–28	$Co + LaCo_{13}(t) + AlCo^{(s)}$	1073
106	4	60	36	$LaCo_{13}(t) + LaCo_5^{(s)} + AlCo^{(s)}$	1073
107	22.2	73.8	4	$La_2Co_7 + LaCo_5^{(s)} + La_2Co_3$	773
108	40	56	4	$La_2Co_3 + La_2Co_{1.7} + LaAl_2^{(s)}$	773
109–112	75	4–21	4–21	$La_3Co + La_3Al$	773
113	64	30	6	$La_3Co + La_2Co_{1.7} + La_3Al$	773
114	46	34	20	$LaAl_2^{(s)} + LaAl + La_2Co_{1.7}$	773
115	84	8	8	$La + La_3Co + La_3Al$	773
116	0	25	75	$Al_5Co_2 + Al_{13}Co_4$	1073

c and t denote the cubic and tetragonal phases of $LaCo_{13-x}Al_x$ respectively, s denotes solid solution.

with $AuCu_3$. The later assessed Al–Co phase diagram of Mcallster [21] included this $AlCo_3$ phase, but its crystal structure and lattice parameters were not reported. This phase was not observed under our experimental conditions.

Table 4
Phase regions and phase compositions in the La–Co–Al ternary system

Phase region	Phase composition
1	$Co + LaCo_{13}^{(s)}$
2	$LaCo_{13}(t) + Co + AlCo^{(s)}$
3	$LaCo_{13}^{(s)} + LaCo_5^{(s)}$
4	$LaCo_5^{(s)} + La_2Co_7$
5	$La_2Co_7 + LaCo_5^{(s)} + La_2Co_3$
6	$La_2Co_3 + LaCo_5^{(s)} + AlCo^{(s)}$
7	$LaCo_{13}(t) + LaCo_5^{(s)} + AlCo^{(s)}$
8	$AlCo^{(s)} + LaAl_2^{(s)} + La_2Co_3$
9	$La_2Co_3 + LaAl_2^{(s)} + La_2Co_{1.7}$
10	$La_2Co_{1.7} + LaAl_2^{(s)} + LaAl$
11	$La_2Co_{1.7} + LaAl + La_3Al$
12	$La_2Co_{1.7} + La_3Al + La_3Co$
13	$La + La_3Co + La_3Al$
14	$LaAl_2^{(s)} + LaAl$
15	$LaAl_2^{(s)} + AlCo^{(s)}$
16	$AlCo^{(s)} + LaCoAl_4 + LaAl_2$
17	$LaCoAl_4 + LaAl_2 + LaAl_3$
18	$AlCo^{(s)} + LaCoAl_4$
19	$AlCo^{(s)} + LaCoAl_4 + Al_5Co_2$
20	$Al_5Co_2 + Al_{13}Co_4 + LaCoAl_4$
21	$Al_{13}Co_4 + Al_9Co_2 + LaCoAl_4$
22	$LaCoAl_4 + Al_9Co_2 + La_3Al_{11}$
23	$Al_9Co_2 + Al + La_3Al_{11}$
24	$LaAl_3 + La_3Al_{11} + LaCoAl_4$

For the $LaCo_{13}$ phase there are two structural types, i.e. cubic phase (c) and tetragonal phase (t).

In the ternary system, the ternary compound $LaCoAl_4$ was reported [22]. It belongs to the monoclinic system with space group *Pmma*, and has also been observed by us. Under our experimental conditions, the following ternary solid solutions were observed. $LaCo_{5-x}Al$ ($x \leq 1$), $LaAl_{2-x}Co_x$ ($x \leq 0.6$) and $LaCo_{13-x}Al_x$. For the $LaCo_{13-x}Al_x$ compounds ($x \leq 2.7$), the X-ray results show that their crystal structures are of the cubic $NaZn_{13}$ type, with lattice parameters $a = 11.345(2)$–$11.473(4)$ Å. The variations in lattice parameter and unit cell volume with Al content are listed in Table 1. At $x = 3$, a structural transition from the cubic $NaZn_{13}$ type to the tetragonal $Ce_2Ni_{17}Si_9$ type occurred. The indexing result indicates that the crystal structure of $LaCo_{10}Al_3$ belongs to the tetragonal space group *I4/mcm*, $Z = 4$. The lattice parameters are $a = 8.085(1)$, $c = 11.624(8)$ Å. A comparison of observed spacings and intensities with calculated ones is made in Table 2. For $x > 3.0$, a certain amount of the AlCo phase and a small amount of the $LaCo_5$ phase existed as secondary phases in addition to the tetragonal phase.

The boundaries of the homogeneity regions of $LaCo_{5-x}Al_x$ and $LaAl_{2-x}Co_x$ were determined using the disappearing phase method, and the results showed that these are $x = 1$ for $LaCo_{5-x}Al_x$ and $x = 0.6$ for $LaAl_{2-x}Co_x$. The $LaCo_{5-x}Al_x$ alloys, according to Ref. [23], are single phase for $x < 1.5$ when annealed at 1273 K for one week. Compared with our

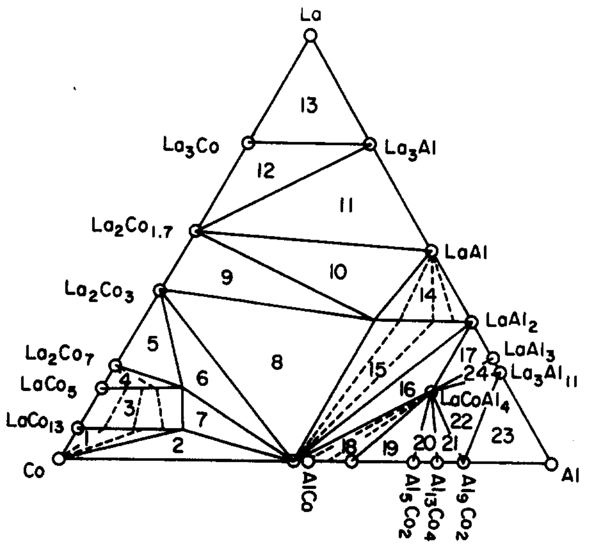

Fig. 1. The subsolidus phase relation diagram of the La–Co–Al ternary system.

results, the homogeneity region seems larger. The reason might be a different annealing temperature and period. In general, homogeneity regions tend to shrink with decreasing annealing temperature. For the cubic $LaCo_{13-x}Al_x$ compounds, we obtained a similar result regarding the homogeneity region. According to the results of Ido et al. [3] the homogeneity region of cubic $LaCo_{13-x}Al_x$ exists for $x < 3.9$, which is larger than our limit ($x \leqslant 2.7$).

A list of alloy compositions and observed phases under the applied annealing conditions of all examined samples is given in Table 3. According to the results of the XRD analysis, the whole ternary La–Co–Al system can be divided into 18 three-phase, six two-phase and four single-phase regions. The phase regions and phase compositions are listed in Table 4. Fig. 1 shows the subsolidus phase relations of the ternary La–Co–Al system.

4. Conclusions

The subsolidus phase relations of the ternary La–Co–Al system have been determined by X-ray powder diffraction. There is one ternary intermetallic compound, $LaCoAl_4$, and three ternary solid solutions, i.e. $LaCo_{5-x}Al_x$ ($x \leqslant 1$), $LaAl_{2-x}Co_x$ ($x \leqslant 0.6$) and $LaCo_{13-x}Al_x$ ($x \leqslant 3$). For $LaCo_{13-x}Al_x$, the crystal structure is cubic $NaZn_{13}$ type for $x \leqslant 2.7$. For $x = 3$, a structural change from a cubic $NaZn_{13}$ to a tetragonal $Ce_2Ni_{17}Si_9$ type structure occurs. The space group of the tetragonal phase is $I4/mcm$, $Z = 4$ and the lattice parameters of the tetragonal $LaCo_{10}Al_3$ are $a = 8.085(1)$, $c = 11.624(8)$ Å. The whole ternary La–Co–Al system can be divided into 18 three-phase, six two-phase and four single-phase regions.

Acknowledgement

This work was supported by the National Natural Science Foundation of China.

References

[1] A. Heidemann, D. Richter and K.H.J. Buschow, *Z. Physik B, 22* (1975) 367.
[2] W.A.J.J. Velge and K.H.J. Buschow, *J. Appl. Phys., 39* (1968) 1717.
[3] H. Ido, J.C. Sohn, F. Pourarian, S.F. Cheng and W.E. Wallace, *J. Appl. Phys., 67* (1990) 4978.
[4] F. Weitzer, K. Hiebl, Yu.N. Grin, P. Rogl and H. Noel, *J. Appl. Phys., 68*(7) (1990) 3504.
[5] G.H. Rao, J.K. Liang, Y.L. Zhang, X.R. Cheng and W.H. Tang, *Appl. Phys. Lett. 64*(13) (1994) 1654.
[6] Weihua Tang, Jingkui Liang, Xiaohua Yan, Guanghui Rao and Sishen Xie, *Phys. Rev. B, 49* (1994) 3864.
[7] Weihua Tang, Jingkui Liang, Xiaolong Chen and Guanghui Rao, *J. Appl. Phys., 76*(7) (1994) 4095.
[8] K.H.J. Buschow and W.A.J.J. Velge, *J. Less-Common Met., 13* (1967) 11.
[9] M. Hansen, *Constitution of Binary Alloys*, McGraw-Hill, New York, 1958.
[10] R.P. Elliott, *Constitution of Binary Alloys, First Supplement*, McGraw-Hill, New York, 1965.
[11] Ralph Hultgren, Pramod D. Desal, Donald T. Hawkins, Molloy Glelley and Kenneth K. Kelley, *Selected Values of the Thermodynamic Properties of Binary Alloys*, University of California, Berkeley, CA, 1973.
[12] W.B. Pearson, *A Handbook of Lattice Spacing and Structure of Metals and Alloys*, Pergamon, London, 1958.
[13] R. Ballou, D. Gignax, R. Lemaire, R. Mendia-Monterroso and J. Schweizer, *J. Magn. Magn. Mater., 54–57* (1986) 499.
[14] D.T. Cromer and A.C. Larson, *Acta Crystallogr., 14* (1961) 1226.
[15] K. Nassau, L.V. Cherry and W.E. Wallace, *Phys. Chem. Solids, 16* (1960) 123.
[16] *JCPDS 21-262*, 1968.
[17] K.H.J. Bushow, *Philips Res. Rep., 20* (1965) 337.
[18] K.H.J. Buschow and J.H.N. van Vucht, *Philips Res. Rep., 22* (1967) 233.
[19] K.A. Gschneidner, Jr. and F.W. Calderwood, *Bull. Alloy. Phase Diagr., 9* (6) (1988).
[20] W.B. Pearson, *A Handbook of Lattice Spacing and Structure of Metals and Alloys*, Supplementary Vol. 2, Pergamon, London, 1967.
[21] A.J. Mcallster, *Bull. Alloy. Phase Diagr., 10* (6) (1989).
[22] *JCPDS 31-7* 1981.
[23] H. Ido, K. Konno, S.F. Cheng, W.E. Wallace and S.G. Sankar, *J. Appl. Phys., 67* (1990) 4638.